Ultralow-loss polycrystalline silicon waveguides and high uniformity 1x12 MMI fanout for 3D photonic integration

David Kwong,[1,*] John Covey,[1] Amir Hosseini,[1] Yang Zhang,[1] Xiaochuan Xu,[1]and Ray T. Chen,[1]

[1]*Microelectronics Research Center, Department of Electrical and Computer Engineering, University of Texas at Austin, 10100 Burnet Rd. Austin, TX 78758, USA*
[*]*david.kwong@utexas.edu*

Abstract: We have investigated the feasibility of multimode polysilicon waveguides to demonstrate the suitability of polysilicon as a candidate for multilayer photonic applications. Solid Phase Crystallization (SPC) with a maximum temperature of 1000°C is used to create polysilicon on thermally grown SiO_2. We then measure the propagation losses for various waveguide widths on both polysilicon and crystalline silicon platforms. We find that as the width increases for polysilicon waveguides, the propagation loss decreases similar to crystalline silicon waveguides. At a waveguide width of 10μm, polysilicon and crystalline silicon waveguides have propagation losses of 0.56dB/cm and 0.31 dB/cm, respectively, indicating there is little bulk absorption from the polysilicon and is the lowest propagation loss for polysilicon demonstrated to date. In addition, the first 1x12 polysilicon MMI is demonstrated with a low insertion loss of −1.29dB and a high uniformity of 1.07dB. These results vindicate the use of polysilicon waveguides of varying widths in photonic integrated circuits.

©2012 Optical Society of America

OCIS codes: (200.4650) Optical Interconnects; (250.5300) Photonic integrated circuits; (130.3120) Integrated optics devices; (230.7370) Waveguides.

References and links

1. N. Sherwood-Droz and M. Lipson, "Scalable 3D dense integration of photonics on bulk silicon," Opt. Express **19**(18), 17758–17765 (2011).
2. C. W. Holzwarth, J. S. Orcutt, H. Li, M. A. Popovic, V. Stojanovic, J. L. Hoyt, R. J. Ram, and H. I. Smith, "Localized substrate removal technique enabling strong-confinement microphotonics in bulk Si CMOS processes," in *Conference on Lasers and Electro-Optics/Quantum Electronics and Laser Science Conference and Photonic Applications Systems Technologies*, OSA Technical Digest (CD) (Optical Society of America, 2008), paper CThKK5.
3. J. Kang, Y. Atsumi, M. Oda, T. Amemiya, N. Nishiyama, and S. Arai, "Low-loss amorphous silicon multilayer waveguides vertically stacked on silicon-on-insulator substrate," Jpn. J. Appl. Phys. **50**, 120208 (2011).
4. S. Zhu, G. Q. Lo, and D. L. Kwong, "Low-loss amorphous silicon wire waveguide for integrated photonics: effect of fabrication process and the thermal stability," Opt. Express **18**(24), 25283–25291 (2010).
5. S. K. Selvaraja, W. Bogaerts, D. Van Thourhout, and M. Schaekers, "Thermal trimming and tuning of hydrogenated amorphous silicon nanophotonic devices," Appl. Phys. Lett. **97**(7), 071120 (2010).
6. T. Kamins, *Polycrystalline Silicon for Integrated Circuits and Displays* 2nd ed. (Kluwer, 1998).
7. S. Zhu, Q. Fang, M. B. Yu, G. Q. Lo, and D. L. Kwong, "Propagation losses in undoped and n-doped polycrystalline silicon wire waveguides," Opt. Express **17**(23), 20891–20899 (2009).
8. Q. Fang, J. F. Song, S. H. Tao, M. B. Yu, G. Q. Lo, and D. L. Kwong, "Low loss (approximately 6.45dB/cm) sub-micron polycrystalline silicon waveguide integrated with efficient SiON waveguide coupler," Opt. Express **16**(9), 6425–6432 (2008).
9. K. Preston, B. Schmidt, and M. Lipson, "Polysilicon photonic resonators for large-scale 3D integration of optical networks," Opt. Express **15**(25), 17283–17290 (2007).
10. K. Preston, S. Manipatruni, A. Gondarenko, C. B. Poitras, and M. Lipson, "Deposited silicon high-speed integrated electro-optic modulator," Opt. Express **17**(7), 5118–5124 (2009).
11. L. Liao, D. R. Lim, A. M. Agarwal, X. Duan, K. K. Lee, and L. C. Kimerling, "Optical transmission losses in polycrystalline silicon strip waveguides: effects of waveguide dimensions, thermal treatment, hydrogen passivation, and wavelength," J. Electron. Mater. **29**(12), 1380–1386 (2000).

12. J. S. Orcutt, S. D. Tang, S. Kramer, K. Mehta, H. Li, V. Stojanović, and R. J. Ram, "Low-loss polysilicon waveguides fabricated in an emulated high-volume electronics process," Opt. Express **20**(7), 7243–7254 (2012).
13. A. Hosseini, D. N. Kwong, Y. Zhang, H. Subbaraman, X. Xu, and R. T. Chen, "1xN multimode interference beam splitter design techniques for on-chip optical interconnections," IEEE J Sel Top Quantum Electron. **17**(3), 510–515 (2011).
14. P. Dumon, W. Bogaerts, D. Van Thourhout, D. Taillaert, R. Baets, J. Wouters, S. Beckx, and P. Jaenen, "Compact wavelength router based on a silicon-on-insulator arrayed waveguide grating pigtailed to a fiber array," Opt. Express **14**(2), 664–669 (2006).
15. M. K. Hatalis and D. W. Greve, "Large grain polycrystalline silicon by low-temperature annealing of low-pressure chemical vapor deposited amorphous silicon films," J. Appl. Phys. **63**(7), 2260–2266 (1988).
16. E. Ibok and S. Garg, "A characterization of the effect of deposition temperature on polysilicon properties," J. Electrochem. Soc. **140**(10), 2927 (1993).
17. Y. Vlasov and S. McNab, "Losses in single-mode silicon-on-insulator strip waveguides and bends," Opt. Express **12**(8), 1622–1631 (2004).
18. M. J. Kobrinsky, B. A. Block, J. Zheng, B. C. Barnett, E. Mohammed, M. Reshotko, F. Robertson, S. List, I. Young, and K. Cadien, "On-chip optical interconnects," ITJ **8**, 129–142 (2004).
19. D. Kwong, Y. Zhang, A. Hosseini, Y. Liu, and R. T. Chen, "1 X 12 even fanout using multimode interference optical beam splitter on silicon nanomembrane," Electron. Lett. **46**(18), 1281–1283 (2010).

1. Introduction

On-chip photonic networks are a promising solution for the interconnect bottleneck in high performance microelectronics. Crystalline silicon-on-insulator (SOI) is the most commonly used photonics platform due to its large index contrast with silicon dioxide ($\Delta n \sim 2.02$), which enables submicron waveguides and small bending radii. In addition, SOI exhibits excellent material properties such as low bulk absorption at telecom wavelengths and high electronic carrier mobility. While crystalline SOI is the most desirable, photonic devices would be restricted to the electronic layer. Furthermore, silicon photonics requires a thick Buried Oxide (BOX) layer (typically a few micrometers) for optical isolation from the substrate, but SOI for electronics requires a thin oxide layer ranging from tens to hundreds of nanometers to allow thermal flow into the substrate [1]. Although it has been shown that SOI for electronics can also be used for photonics [2], it comes generally at the cost of more real estate and adds greater complexity and cost to the standard CMOS fabrication process. A multi-layer platform would enable photonic device versatility, as footprint and separation issues are mitigated.

In order to maximize such a platform's design flexibility, CMOS compatible silicon deposition methods are strongly desired. As it is not currently possible to deposit crystalline silicon, alternative materials must be considered. Silicon nitride is a low loss material that has been used for multilayer photonic integration [1], but its lower index contrast increases device footprint, and it also lacks any mechanism for high-speed modulation, limiting nitride to either passive devices or slower devices using the thermo-optic (TO) effect. Hydrogenated amorphous silicon deposited by Plasma-Enhanced Chemical Vapor Deposition (PECVD) is a low loss material that has been used in multilayer stacks [3], but sufficient and stable hydrogenation of the silicon dangling bonds are critical to maintaining its low loss property. Zhu et al have demonstrated that the propagation loss for hydrogenated amorphous silicon waveguides starts to increase rapidly at temperatures above 300°C [4], and Selvaraja et al have shown that the refractive index change measured from a Mach-Zehnder Interferometer (MZI) starts to occur at 200°C [5]. In addition to thermal stability of hydrogenated amorphous silicon, another significant challenge is that the charge mobility is very low due to the amorphous structure of the film, thereby limiting its application in high-speed applications.

Deposition of polycrystalline silicon (polysilicon) is a mature, CMOS compatible process that is easy to deposit on a variety of substrates. In addition, it can be easily doped to realize electrically active photonic devices due to its relatively high ($\sim 100 \text{cm}^2/\text{V-s}$) [6] electronic carrier mobility. Propagation loss has remained a significant challenge for polysilicon waveguides, which is dominated by scattering and absorption at the polycrystalline grain boundaries. Low loss ($\sim 6.45 \text{dB/cm}$) single mode polysilicon waveguides [7, 8], high quality factor ring resonators [9], and high speed electro-optic modulators [10] formed by Solid Phase Crystallization (SPC) of Low Pressure Chemical Vapor Deposition (LPCVD)

amorphous silicon have been demonstrated. Compared to direct deposition of LPCVD polysilicon, SPC of LPCVD amorphous silicon yields superior film qualities, such as smoother surfaces to reduce interfacial scattering and larger grains that result in fewer absorbing and scattering boundaries, further lowering the propagation loss [11].

To date, photonic polysilicon research has focused on waveguides and devices in the single mode region with thicknesses of 200-250nm and widths of 300-500nm, where narrower waveguides result in lower loss due to less confinement of light in the polysilicon core, indicating that attenuation is dominated by bulk loss [7]. Indeed, efforts to further reduce the overlap of the optical mode with the waveguide cross section have been made by forming polysilicon waveguides in the same step as the polysilicon transistor gate for electronics, resulting in core geometries of 120nm X 350nm and a propagation loss of 6.2 dB/cm at 1550nm [12]. Unfortunately, little work exists for wider, multimode polysilicon devices. Liao et al have reported that thicker and wider polysilicon waveguides suffer from higher propagation losses due to increased optical confinement [11]. However, for key photonic components such as multimode interference couplers (MMI) for beam splitting and arrayed waveguide gratings (AWG) for wavelength division multiplexing (WDM), device dimensions can span tens to hundreds of microns in width [13, 14]. Characterizing the loss of polysilicon at such widths is necessary to determine if these devices can be formed without prohibitively high losses.

In this paper, we demonstrate the lowest propagation loss to date of 0.56dB/cm to date in polysilicon waveguides, as well as the first 1x12 polysilicon MMI with an insertion loss of −1.29dB and a uniformity of 1.07dB.

2. Design and Fabrication

We have used the beam propagation method (BPM) from Rsoft to simulate 10μm wide waveguides for both crystalline silicon and polysilicon with grain boundaries, which is shown in Fig. 1(a) and 1(b), respectively. Figure 1(a) shows the 10μm wide crystalline silicon waveguide excited by the fundamental mode, which propagates through the waveguide undisturbed. In contrast, a polysilicon waveguide is simulated by adding grain boundaries. The grain boundaries scatter light into higher order modes that are still guided by the wide waveguide. For narrower waveguides, the grain boundaries scatter light into radiative modes, as higher order modes are not guided. Therefore, the number of guided modes in a given waveguide geometry determines the propagation loss due to grain boundary scattering.
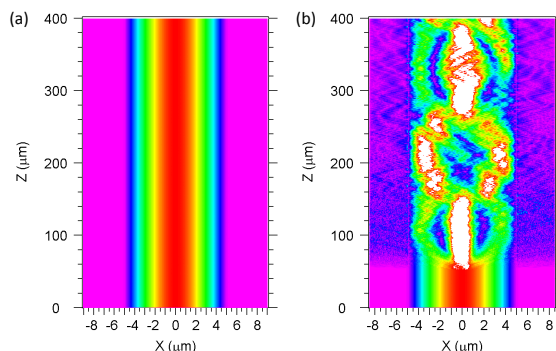

Fig. 1. Beam Propagation Method simulation of 10μm waveguide for (a) crystalline silicon and (b) polysilicon with grain boundaries.

In order to investigate the effect of the waveguide width on the propagation loss of polysilicon waveguides, the waveguide width is varied by using the structure shown in Fig. 2(a). Grating couplers are used for input and output coupling. Due to the phase matching condition for grating couplers, the higher order modes excited by polysilicon grain boundary scattering will diffract out at different angles due to their different propagation constants. The details of this grating coupler will be reported separately. After the grating coupler, we first

adiabatically taper all waveguide widths to 500 nm in order to filter out higher order modes and achieve single mode propagation. The waveguide is then adiabatically tapered to the desired waveguide width, which ranges from 400 nm to 10 µm. After 5 mm of propagation, all waveguides are then tapered back to the output waveguide width. The same structures are also fabricated on crystalline silicon as a reference. By having the exact same structure and fabrication process, our results can only arise from the differences between the two materials.

In addition, we also designed a 1x12 Multimode Interference (MMI) optical beam splitter to further demonstrate large multimode polysilicon devices. The length and width of the multimode region are $L_{MMI} = 563.4$ µm and $W_{MMI} = 60$ µm respectively. The input and access waveguides are both 2.6 µm wide. To clearly resolve the individual output spots in the near field, a fanout design was used to separate the 12 MMI output channels to 30 µm. A schematic of the 1x12 MMI can be seen in Fig. 2(b).
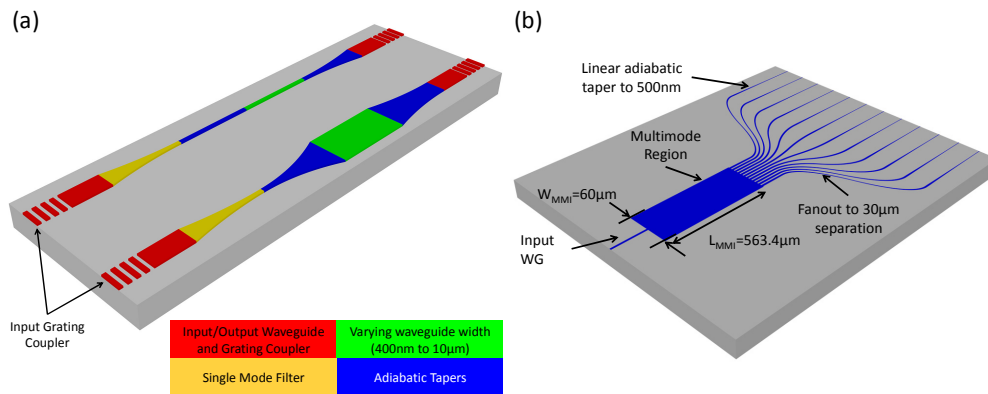

Fig. 2. (a) Schematic of waveguide structure. Not drawn to scale. (b) Schematic of 1x12 polysilicon MMI.

In our experiment, we thermally oxidize a bare silicon wafer to create 2.0µm of SiO_2 which acts as the BOX layer and is thick enough to prevent optical leakage into the substrate. Afterwards, a 250nm thick layer of amorphous silicon was deposited using Low Pressure Chemical Vapor Deposition (LPCVD) at 550°C. From [15], we find that the deposition rate should be sufficiently high to minimize the number of nucleation sites, which results in increased grain size. Consequently, we use an increased silane gas flow of 150sccm to achieve a deposition rate of 3.3nm/minute. After the amorphous silicon deposition, we briefly dip the wafers in Piranha solution to form a native oxide layer. This thin native oxide layer stabilizes the top surface of the amorphous silicon and prevents increased surface roughness during future anneal treatments [16]. The wafers are then annealed using a two-step annealing process. The first anneal is a low temperature anneal that is done at 600°C N_2 for 40 hours, and the purpose of this anneal is for gradual grain nucleation, which results in large grains. The second anneal is a 5 hour 1000°C also in N_2, and this step is to crystallize the individual polysilicon grains.

In order to estimate our grain size, we use dry oxidation at 900°C for 30 minutes to oxidize the top surface of our polysilicon film. Because polysilicon grains will preferentially oxidize along grain boundaries, we can use Buffered Oxide Etch (BOE) to remove the oxide and then use Scanning Electron Microscopy (SEM) to visualize our grains. A picture of such an SEM image is shown in Fig. 3(a), and we estimate the grain sizes to be ~300nm.

The waveguides were patterned using electron beam lithography and Reactive Ion Etching (RIE). Afterwards, a 1µm thick film of SiO_2 for top cladding was deposited using PECVD. A cross section view of a single mode polysilicon waveguide is shown in Fig. 3(b), and a microscope image of the 1x12 MMI is shown in Fig. 3(c).
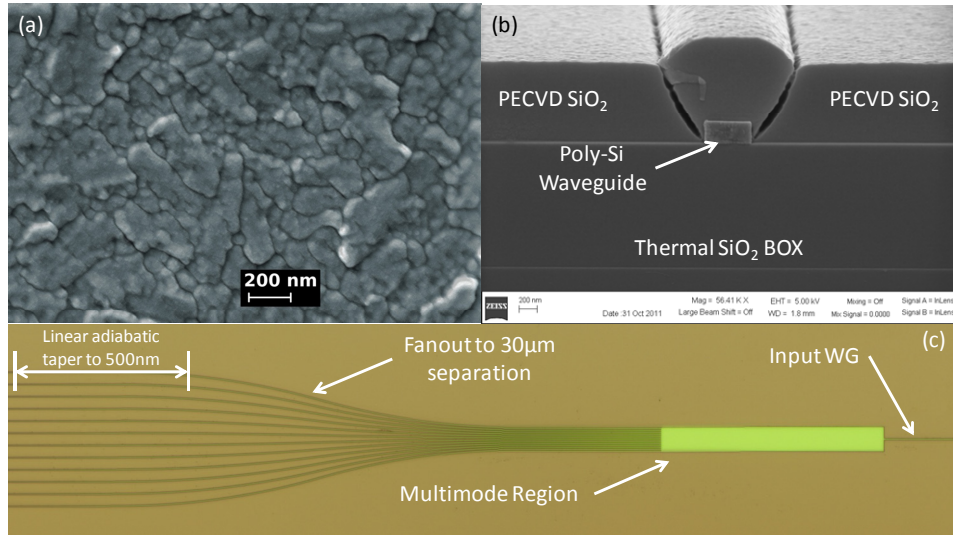
Fig. 3. (a) Top down SEM image of polysilicon grains after oxidation and BOE, (b) cross sectional SEM of a single mode polysilicon waveguide and (c) microscope image of the completed 1x12 MMI.

3. Results and Analysis

Transverse Electric (TE) polarized light at 1550nm was coupled into the input grating coupler using a polarization maintaining fiber (PMF) and collected from the output grating by standard single mode fiber (SMF). The propagation loss of various waveguide widths for both crystalline and polysilicon are shown below in Fig. 4.
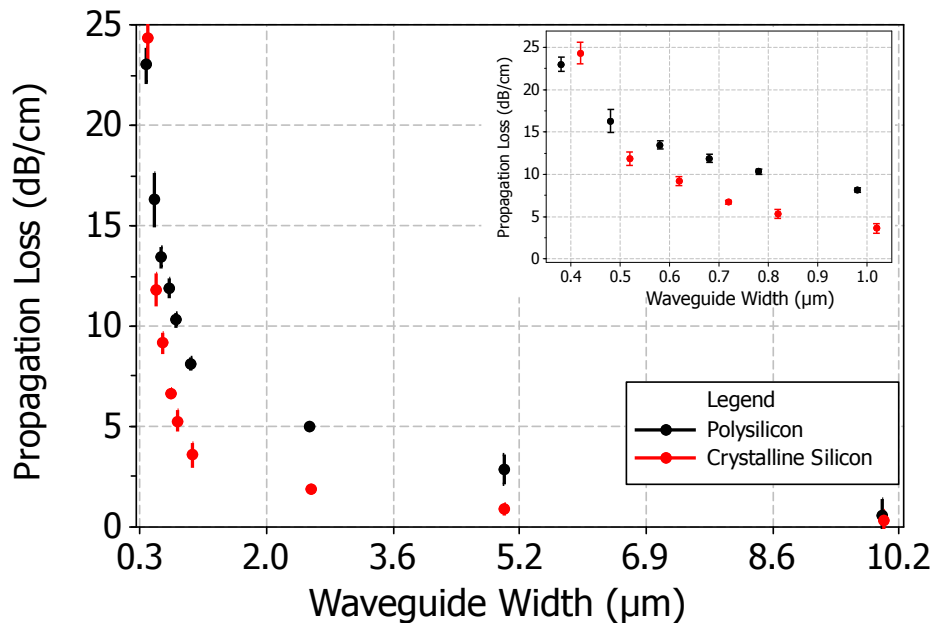

Fig. 4. Propagation loss of various polysilicon and crystalline silicon waveguide widths. Inset shows a close up view of 0.4μm to 1 μm. Standard error bars are given for each data measurement.

The propagation loss decreases for both crystalline silicon and polysilicon as the waveguide width increases. At a waveguide width of 400nm, the propagation losses of crystalline and polysilicon are virtually the same, but as the waveguide width increases, the loss difference between the two also increases. For waveguide widths above 2.5μm, the difference in propagation loss between crystalline and polysilicon decreases until they have nearly identical propagation losses at 10μm. For crystalline silicon, this behavior is well known and is due to decreasing sidewall interaction of the fundamental mode of the waveguide [17]. However, the grain boundaries present in polysilicon cause scattering to either radiation modes or higher order modes depending on whether the waveguide width supports the higher modes. This scattering into higher order modes causes the additional loss between polysilicon and crystalline waveguides of the same width. The presence of the higher order modes has been experimentally confirmed using the grating coupler, as we observed uniform output power throughout a range of different fiber tilt angles. This is due to the presence of multiple modes, each with their respective propagation constants which are diffracted out at different angles. The details of this result will be reported in a separate publication.

It is important to note that at a 10μm waveguide width, both polysilicon and crystalline silicon waveguides have the lowest losses of 0.56dB/cm and 0.31dB/cm, respectively. To our knowledge, this value is the lowest propagation loss for a polysilicon waveguide to date. Furthermore, it indicates that there is very little bulk absorption from the polysilicon grain boundaries. This behavior of decreasing propagation loss with increasing waveguide width validates the use of large polysilicon waveguides in photonic integrated circuits whenever bandwidth-density is affordable [18].

We fabricated the first polysilicon based 1x12 MMI and experimentally confirmed the functionality of such a 60μm wide polysilicon device. As before, TE polarized light at 1550nm was coupled into the 1x12 MMI. Using an IR camera, 12 output spots are imaged from the MMI fanout, which are shown in Fig. 5(a). To characterize the performance of this 1x12 MMI, we used lensed fiber to collect each of the 12 output intensities, which is shown in Fig. 5(b). The performance of an MMI can be described by output uniformity and insertion loss. The uniformity is calculated as $10\log\left(I_{max}/I_{min}\right)$, where I_{max} and I_{min} are the maximum and minimum output intensities of the MMI, respectively. The insertion loss of the MMI is defined as $-10\log\left(\sum I_i / I_{in}\right)$, where I_i is the output intensity of the ith output channel, and I_{in} is the intensity of a straight waveguide with the same dimensions of the MMI input waveguide. For our polysilicon 1x12 MMI, we determine a uniformity of 1.07dB and an insertion loss of -1.29dB. The insertion loss is a negative number because the output intensity of the input waveguide used for normalization is lower than the sum of the MMI output intensities. This is due to the presence of the multimode region of the MMI, which is 60μm wide and 563.4μm long and has a much lower loss compared to the much narrower input waveguide. We have previously demonstrated a 1x12 MMI on crystalline silicon with comparable performance [19].
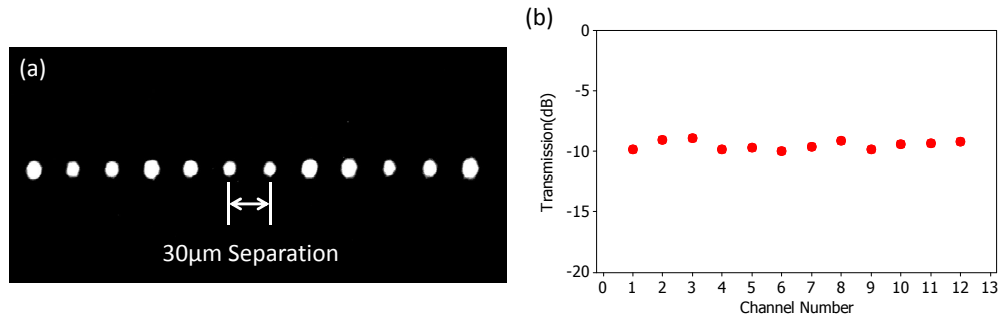
Fig. 5. (a) IR image of the 12 output spots from 1x12 MMI fanout. (b) Output intensities of the 1x12 polysilicon MMI.

4. Conclusion

We have investigated the feasibility of multimode polysilicon waveguides to demonstrate the suitability of polysilicon as a candidate for multilayer photonic applications. SPC with a maximum temperature of 1000°C is used to create polysilicon on thermal SiO_2. We then measure the propagation losses for various waveguide widths on both polysilicon and crystalline silicon platforms. We find that as the width increases for polysilicon waveguides, the propagation loss decreases similarly to crystalline silicon waveguides. The difference in loss between the two platforms for a given waveguide width is due to the scattering from the polysilicon grain boundaries, which excites higher order modes. Depending on the waveguide width, these modes either propagate as higher order modes or are lost as radiation modes. We also find that at a waveguide width of 10µm, the polysilicon propagation loss of 0.56dB/cm is very close to the crystalline silicon propagation loss of 0.31dB/cm, indicating that there is little bulk absorption from the polysilicon. This result validates the use of polysilicon waveguides in photonic integrated circuits. We further demonstrate this with a 1x12 polysilicon MMI that has a low insertion loss of −1.29dB and a high uniformity of 1.07dB. Together, we present the lowest propagation loss for polysilicon waveguides to date of 0.56dB/cm as well as the first 1x12 polysilicon MMI.

Acknowledgments